IEEE Access
Multidisciplinary | Rapid Review | Open Access Journal

Received 22 December 2024, accepted 9 January 2025, date of publication 14 January 2025, date of current version 17 January 2025.

Digital Object Identifier 10.1109/ACCESS.2025.3529458

RESEARCH ARTICLE

Design of Single Feed, Dual-Band Circularly Polarized Quad-Mode Slot Antenna Using Coupled Mode Theory

MEKALADEVI V, (Graduate Student Member, IEEE), AND NATARAJAMANI S, (Member, IEEE)
Department of Electronics and Communication Engineering, Amrita School of Engineering, Amrita Vishwa Vidyapeetham, Coimbatore 641112, India
Corresponding author: Natarajamani S (s_natarajamani@cb.amrita.edu)

ABSTRACT In this article, a dual-band, dual-sense circularly polarized (CP) rectangular slot antenna with folded slots, fed by a microstrip line, is presented for GPS applications at 1575.4 MHz (L1) and 1227.5 MHz (L2). The excitation of the rectangular slot antenna maintains a small frequency ratio by generating two modes at closely spaced frequencies through characteristic mode analysis (CMA) and coupling mode theory (CMT). Dual circular polarization is then achieved by creating two orthogonal modes with respect to the fundamental modes by inserting two folded slots at angles of $-45°$ and $45°$ relative to the tilted arm of the rectangular slot antenna. The proposed antenna has $100 \times 100 \times 1.6\ mm^3$ dimensions and radiates right-hand CP (RHCP) in the L1 band and left-hand CP (LHCP) in the L2 band. The measured impedance bandwidth is 3.6 % (1615-1675 MHz) for L1 and 26.7 % (1055-1380 MHz) for L2. The axial ratio bandwidth (ARBW) is observed as 3.2 % (1565-1616 MHz) for L1 and 4.04 % (1212-1262 MHz) for L2, with a maximum gain of 4.1 dBic and 3.8 dBic, respectively.

INDEX TERMS Characteristic mode analysis (CMA), circularly polarized (CP), coupled mode theory (CMT), dual-band, folded slots, slot antenna.

I. INTRODUCTION

The Global Positioning System (GPS) has revolutionized communication through advancements in modern technology. GPS, a part of the Global Navigation Satellite System (GNSS), uses a constellation of medium Earth orbit satellites to transmit microwave signals, allowing receivers to accurately determine the user's location, speed, and time. GPS provides users worldwide with precise location and timing information. It operates on two frequency bands, L_1 and L_2, to enhance satellite communication and monitoring. A fundamental challenge in antenna design is that multiple antenna usage, required to cover different frequency bands, creates the problem of mutual coupling, which reduces system efficiency. This issue can be mitigated by designing a single antenna that resonates at dual frequencies with dual-sense circular polarization. Moreover, right-hand circular polarization (RHCP) and left-hand circular polarization (LHCP) are required to minimize interference for the L_1 and L_2 frequency bands. Consequently, this application demands a simple, low-profile, compact antenna structure with dual-sense circular polarization [1], [2], [3], [4].

Several designs have been reported with single and stacked layers, employing simple and complex feeding mechanisms. Patch antennas with simple feed networks and loaded with slits and slots have been explored to achieve dual-band circular polarization (CP); however, these designs often exhibit large frequency ratios [5]. Although stacking patches on different substrates can reduce the frequency ratio, this approach fails to ensure stable gain across the operating frequency range [6]. Maintaining a consistent frequency ratio remains a significant challenge in the design of dual CP antennas. Stacked patch structures with complex feeds have been investigated to address this issue [7]. While annular ring slot antennas have been explored for dual CP, they often demonstrate large frequency ratios [8].

The associate editor coordinating the review of this manuscript and approving it for publication was Giovanni Angiulli.

Aperture-coupled feeds in stacked patch configurations have been used to achieve smaller frequency ratios, but these designs suffer from low front-to-back ratios [9]. Slot antennas have been studied to minimize out-of-band interference and use restricted frequency bands better. These antennas are appealing due to their simple structure, compactness, and stable performance [10], [11]. A wide-slot antenna was proposed for dual CP by combining slot and monopole modes to achieve dual-band CP radiation [12]. However, these antennas often operate with a large frequency ratio. To address this issue, narrow-slot antennas with various slot shapes have been considered. Despite the addition of strips and slits to the patch, achieving frequency flexibility across the dual resonant frequencies remains challenging, as reported in [13] and [14].

By altering the slot shape to a spiral and combining it with two deformed monopoles, a small frequency ratio was achieved [15]. Substrate Integrated Waveguide (SIW) annular slot antennas have been reported to achieve dual CP with a small frequency ratio; however, they require a large matching circuit area for impedance matching [16]. To reduce radiator spacing, narrow-slot antennas have been investigated. Narrow-slot antennas with differential feeds were proposed to achieve dual-band linear polarization (LP) using the multimode resonant concept, which enhances bandwidth and reshapes the radiation pattern [17]. The multimode resonance concept has also been applied to achieve dual-band CP by designing spiral slot radiators with annular slots fed by microstrip lines [18].

Characteristic Mode Analysis (CMA) has been used for decades to characterize radiating structures. Initially, the concept of CMA was proposed by [19] and later redefined by [20], CMA has been applied in wideband and dual-band applications to analyze the existence of natural modes in radiating structures. A U-slot patch antenna was analyzed using CMA to interpret coupled and uncoupled modes, achieving a wide impedance bandwidth [21], [22]. The importance of excitation in triggering modes within a nearby frequency range was discussed in [23]. The concept described in [24] explores the characteristic behavior of coupled systems in creating resonant modes. In [25], the exchange of characteristics between in-phase and anti-phase modes was addressed, explaining intermodal energy alteration.

In [26], narrow slot antennas with folded stubs were realized for dual CP higher-order modes were utilized for dual CP making it unsuitable for low-frequency applications. A double-layered annular ring patch antenna with crossed slots, fed by a coaxial feed, was proposed for GAGAN receivers, achieving dual-band resonance with dual polarization for both bands [27]. However, the design is complex due to the insertion of slits and vias in a multilayer structure. A stub-loaded annular ring patch antenna with CP was proposed in a 2 × 2 array configuration, and a monopole antenna was proposed for MIMO satellite and MIMO mobile terminal applications, respectively [28], [29]. An S-shaped slot was created from a narrow-slot antenna to realize a compact antenna structure with high cross-polarization and low gain [30].

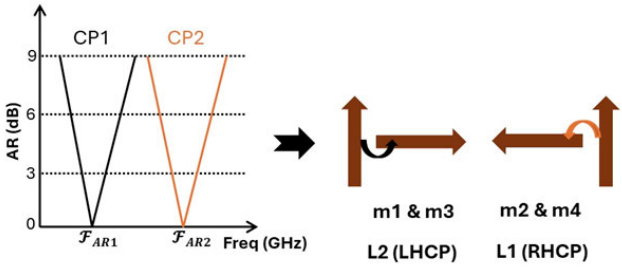

FIGURE 1. Expected dual CP performance and dual orthogonal polarization with rotations.

In [31], a compact annular ring slot antenna with a proximity-coupled feed was proposed for dual CP but demonstrated limited performance in terms of gain and axial ratio bandwidth. The array structure implemented in [32] was larger in size, with low axial ratio bandwidth (ARBW) and small frequency ratio. Folded slots are employed in antenna miniaturization to maintain similar radiation patterns for the first and second resonance modes [33]. In [34], the quad-mode technique is proposed to achieve dual sense CP but uses a multilayer with aperture-coupled feed. In this work, the concepts of Characteristic Mode Analysis (CMA) and Coupled Mode Theory (CMT) are employed to achieve a small frequency ratio, while folded slots are utilized to attain dual-band circular polarization (CP) for GPS applications. A rectangular slot, combined with folded slots at appropriate angles, produces dual-band, dual-sense CP radiation. The CMT concept is used to generate resonances at L1 and L2 with the required frequency ratio by properly exciting the radiating structure with a microstrip line feed. This approach is explored for the first time in the design of a dual-band CP antenna with a single layer, single feed, and single radiating element. The work is organized as follows: Section II explains the working principle and technique of CP antennas, Section III describes the proposed antenna geometry and working principle, and Section IV presents the results and discussion.

II. CP ANTENNA WORKING PRINCIPLE

In this work, an effective approach is proposed for designing a dual-band, dual circularly polarized (CP) slot antenna by simultaneously exciting two resonant modes (m_1 and m_2) with in-phase and anti-phase characteristics in a nearby frequency range, thereby maintaining a small frequency ratio suitable for GPS applications. In addition to the fundamental modes, two orthogonal modes (m_3 and m_4) are created by inserting folded slots with opposite rotations (m_1 with m_3 and m_2 with m_4), and the expected axial ratio is shown in Fig. 1. Thus, dual-sense circular polarization will be achieved with a single-layer, single-feed antenna structure.

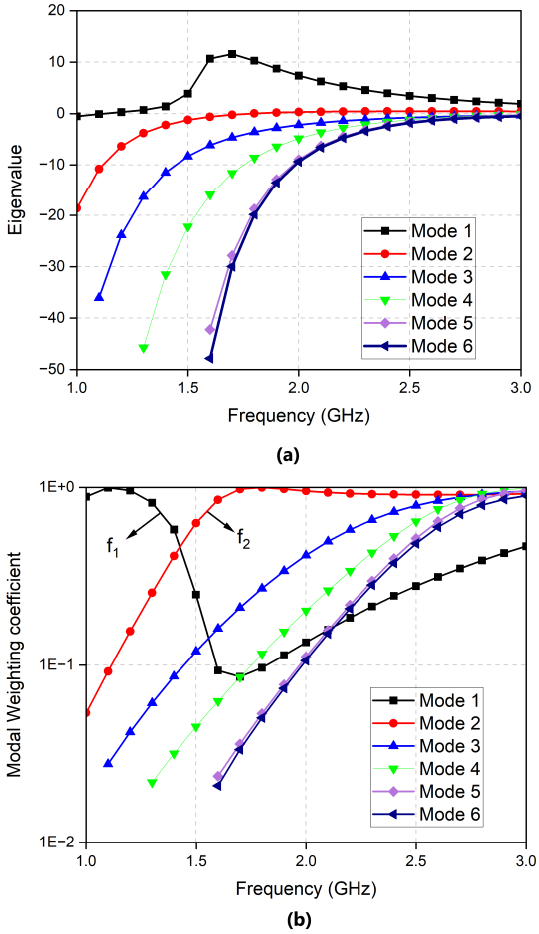

FIGURE 2. (a) Rectangular slot eigenvalues (b) Modal weighting coefficient values show mode 1 and mode 2 are coupled modes.

A. CMA TECHNIQUE

CMA is the technique used to study the radiating properties of any arbitrarily shaped structures and to study the natural modes of the radiating structure. Characteristic modes can be analyzed from the linear weighted sum of the eigenvalue function [20], as shown in equation (1).

$$X(J_n) = \lambda_n R(J_n) \tag{1}$$

where λ_n and J_n are the eigen values and eigen currents, R and X are the real and imaginary parts of the impedance operator.

$$MS = \left|\frac{1}{1 + j\lambda_n}\right| \tag{2}$$

Modal significance can be computed from equation (2). The modes can be analyzed in any arbitrarily shaped structure, either with a modal weighting coefficient or an eigenvalue function. According to equation (2), a modal significant value of 1 with $\lambda_n = 0$ represents the radiating mode, whereas negative and positive values represent the capacitive and inductive nature, respectively.

$$CA = 180^\circ - \arctan(\lambda_n) \tag{3}$$

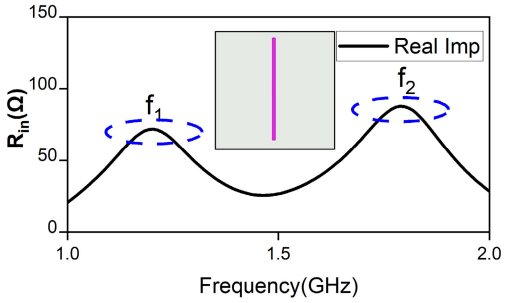

FIGURE 3. Impedance plot for rectangular slot.

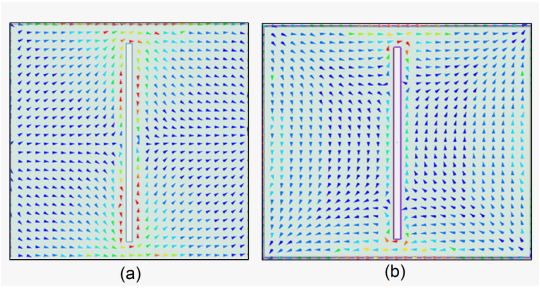

FIGURE 4. Current distribution at (a) 1.2 GHz, (b) 1.8 GHz.

Characteristic angle (CA) provides the phase difference between the characteristic current and the field, and its mathematical function is given in equation (3). If the phase difference is 90°, the generated mode is at the resonance frequency. If the phase difference is between 90° and 180°, the generated mode is inductive, otherwise it is capacitive in nature. Both CA and MS are used to differentiate between radiating and non-radiating modes and to identify the coupled modes.

B. CMT TECHNIQUE

Coupled Mode Theory (CMT) is a subpart of CMA that explains the coupling between the two resonant modes. A coupled system exhibits a lower, in-phase resonant frequency and a higher, out-of-phase resonant frequency with similar radiation patterns. The amount of coupling determines the separation between the resonant frequencies. The eigenvalues and modal significance obtained from the CMA analysis are shown in Fig.2. There are six modes generated over the frequency range 1-3 GHz, but only modes 1 and 2 intersect, exhibiting coupled modes at frequencies at 1.2 GHz and 1.8 GHz, with a modal significance of 1. This method is particularly useful when two resonant modes are excited at nearby frequencies to achieve a small frequency ratio. To maintain the same frequency ratio and resonant mode frequencies, the feed must be properly positioned and excited, as outlined in [24]. The following equations describe the coupling between the frequencies.

$$\omega_+ = \omega + |K| \tag{4}$$

$$\omega_- = \omega + |K| \tag{5}$$

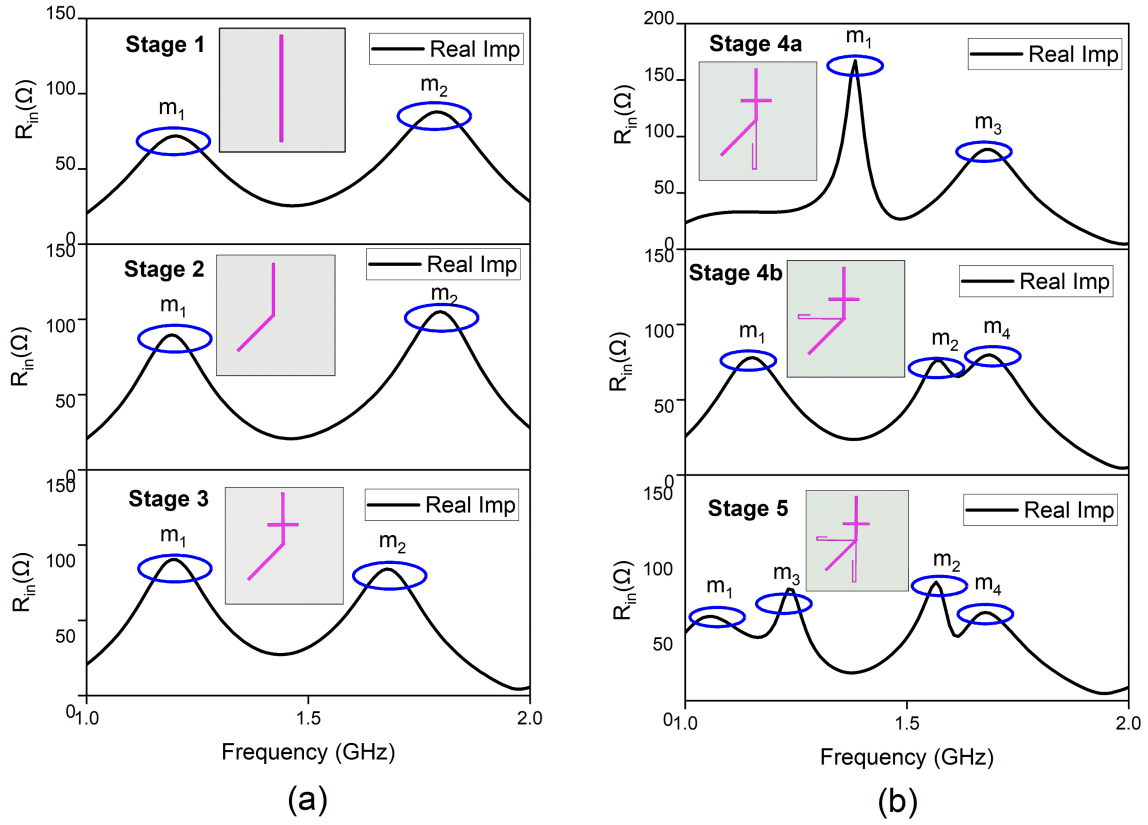

FIGURE 5. Creation of orthogonal mode pairs (a) Stage 1-3 (b) Stage 4-5.

where ω_+ and ω_- are the higher and lower coupled angular frequencies, ω is the angular frequency at which two coupled resonances meet, and K is the coupling coefficient.

When the antenna is fed with microstripline, the modes are observed at the same frequencies (f_1 and f_2) where the CMA analysis indicated the resonant modes, as shown in Fig. 3.

The excitation is applied at the locations of maximum electric field to activate the coupled modes at the desired frequencies. The simulated current distribution plot from the CMA analysis for the coupled modes is shown in Fig. 4. The current distributions at 1.2 GHz and 1.8 GHz for modes 1 and 2, with in-phase and out-of-phase behavior, are depicted.

C. ORTHOGONAL MODES CREATION FOR DUAL CP OPERATION

To achieve dual CP at the desired frequencies, it is necessary to create pairs of orthogonal modes without shifting the resonant modes. In this approach, five design evolutions are discussed to obtain dual CP, and each stage is analyzed in terms of Z_{11}, representing the modes with their peak values. The evolution begins with stage 1 which features a conventional rectangular slot antenna fed by a microstrip line. The coupled modes (m_1 and m_2) are observed at peak values of 1.20 GHz and 1.8 GHz, respectively.

D. EVOLUTIONARY STAGES

Evolutionary stages are shown in Fig. 5. In stage 2, to initiate the creation of orthogonal modes, the conventional slot is divided into two halves. One half of the slot is tilted at an angle of 45°, while the other half remains at an angle of 0°. This approach maintains the radiating mode frequencies although a slight change is observed in the impedance magnitude.

In Stage 3, impedance matching is prioritized. A horizontal slot with a length of 25 mm and a width of 2.5 mm is placed 25 mm away from one arm of the rectangular slot to achieve impedance matching. Due to field perturbation, the radiating modes merge, resulting in a wide impedance bandwidth of 500 MHz, with the first and second resonances occurring at 1.275 GHz and 1.62 GHz, respectively.

In stage 4a, an orthogonal mode (m_3) is created by placing a folded slot at an angle of $-45°$ relative to the tilted arm. The folded slot dimensions are calculated from [33]. The Z_{11} plot confirms that an additional mode (m_3) is created close to m_1, resulting in impedance bandwidths of 100 MHz and 216 MHz, with resonances at 1.15 GHz and 1.6 GHz, respectively. The folded slot length is set to 64.05 mm, corresponding to half of the guided wavelength at the resonance frequency at which the mode is created. LHCP

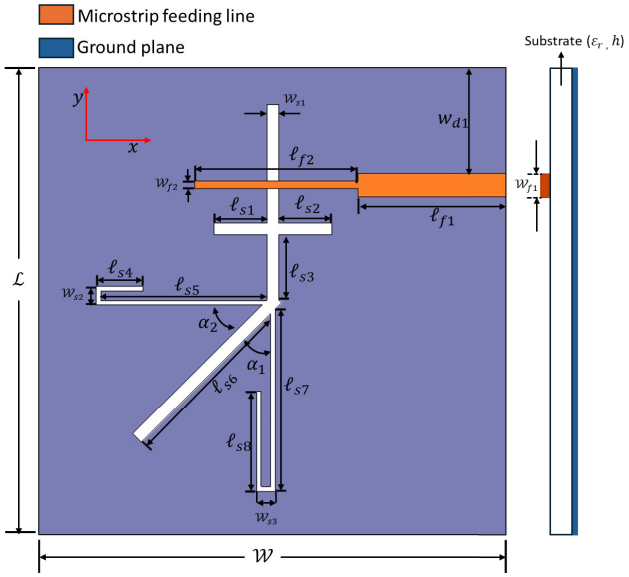

FIGURE 6. Proposed antenna geometry.

at L_2 is achieved with an axial ratio of 2.71 dB and a 3 dB ARBW of 30 MHz.

In alignment with stage 4b, another folded slot is designed to create an additional orthogonal mode (m_4) near the L_1 band. This slot is placed at an angle of 45° relative to the tilted arm, thereby creating RHCP at L_1. The folded slot length is 49.2 mm, as referenced in Stage 4. The minimum axial ratio is observed at 1.575 GHz with a bandwidth of 25 MHz. The resonances are at 1.2 GHz and 1.61 GHz, with impedance bandwidths of 186 MHz and 160 MHz, respectively. The proposed antenna design is achieved by

TABLE 1. Optimized parameters.

Parameter	W	L	l_{s1}	l_{s2}	l_{s3}	l_{s4}
value (mm)	100	100	11.25	11.25	14	10
Parameter	l_{s5}	l_{s6}	l_{s7}	l_{s8}	w_{d1}	w_{s1}
value (mm)	35.2	27.5	38.8	21.25	22.54	2.5
Parameter	w_{s2}	w_{s3}	w_{f1}	w_{f2}	l_{f1}	l_{f2}
value (mm)	4	4	4.92	1.6	34.6	32

combining the two folded slots at angles of 45° and −45° and creating quad modes to obtain dual CP at the L_1 and L_2 bands, thereby generating RHCP and LHCP.

III. PROPOSED ANTENNA GEOMETRY AND WORKING PRINCIPLE

The conventional rectangular slot antenna has a length of 84 mm and a width of 2.5 mm. It is etched on the bottom side of a dielectric substrate with a relative permittivity of 2.2 and a thickness of 1.6 mm. A microstrip line is placed on top of the substrate to feed the radiating element. The proposed antenna is designed and simulated using Ansys High-Frequency Structure Simulator (HFSS R2024). The slot

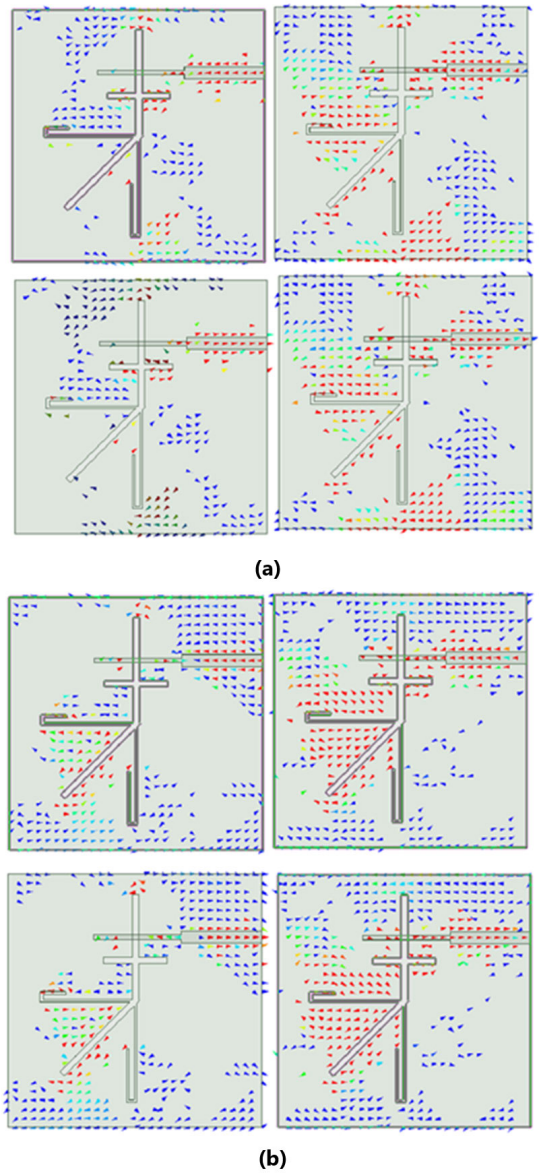

FIGURE 7. (a) Surface current distribution 1.227 GHz, (b) Surface current distribution 1.575 GHz.

antenna dimensions are calculated from [11] and are given as:

$$L_s = \lambda_g/2. \tag{6}$$

$$\lambda_g = \lambda_0/\sqrt{\epsilon_r}. \tag{7}$$

where L_s is the slot length, λ_g is the guided wavelength at the fundamental mode frequency. ϵ_r represents the relative permittivity of the substrate. The proposed antenna geometry is shown in Fig. 6, and the corresponding antenna geometries are listed in Table 1. The inclined angles of folded slots are $\alpha_1 = -45°$ and $\alpha_2 = 45°$, respectively.

A. CP MECHANISM

The circular polarization (CP) of an antenna is validated through its current distribution and is determined by the

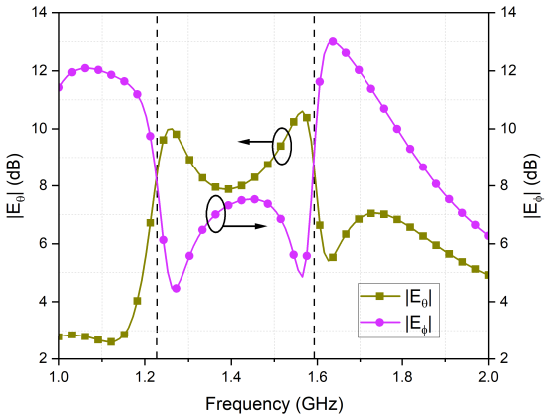

FIGURE 8. Magnitude of E_θ and E_ϕ of proposed antenna.

radiating structure and feed position. The direction in which the electric field vector rotates determines whether it exhibits left-hand circular polarization (LHCP) or right-hand circular polarization (RHCP). The simulated current distributions, shown in Fig. 7, are observed at different angles of 0°, 90°, 180°, and 270°. From the current rotation angle in Fig. 7, it is evident that the radiating element alternates between the clockwise and anticlockwise directions to generate RHCP and LHCP at two resonance frequencies. The electric field vector rotates in an anti-clockwise direction at L_2 and in a clockwise direction at L_1.

Further, the circular polarization mechanism is validated with the simulated magnitudes of the broadside E_θ and E_ϕ components of the proposed antennas as a function of frequency is shown in Fig.8. It is evident that the magnitudes of these fields are equal at around 1.227 GHz and 1.575 GHz. This plot helps in validating the CP at dual bands. Therefore, left-hand circular polarization (LHCP) and right-hand circular polarization (RHCP) are excited at two different frequencies, even though they are close together, maintaining a good isolation between them.

B. DESIGN PROCEDURE

The evolution mechanism of the dual CP slot antenna, a generalized design guideline is summarized in the four steps.

- Step 1: Choose the rectangular slot length according to the first resonance frequency of $\lambda_g/2$.
- Step 2: Divide the slot into two equal arms, rotate one of the arms at an angle of 45°, and introduce a horizontal slot slightly greater than $\lambda_g/4$ for impedance matching.
- Step 3: Insert a folded slot dimension of $\lambda_g/4$ at an angle of $-45°$ with respect to the tilted arm to create an orthogonal mode at the L_2 band.
- Step 4: Insert a folded slot dimension of $\lambda_g/4$ at an angle of 45° with respect to the tilted arm to create an orthogonal mode at the L_1 band.

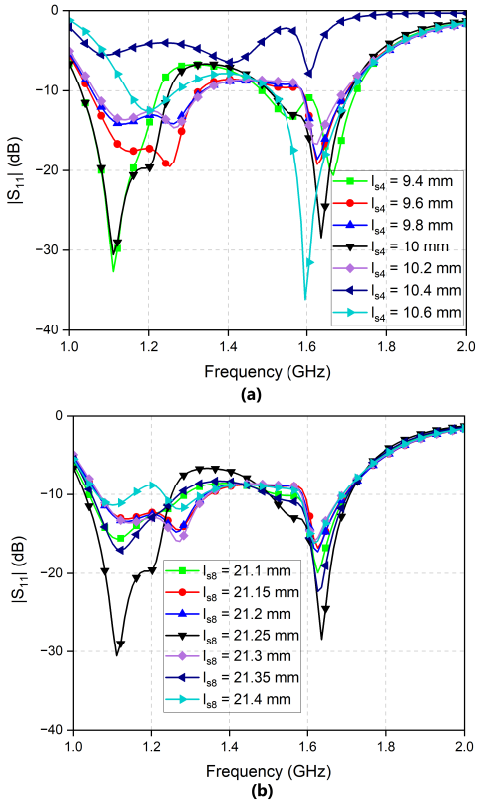

FIGURE 9. Effect of design parameters a) $l_{s4} = 10mm$, b) $l_{s8} = 21.25\ mm$.

C. PARAMETRIC ANALYSIS

The performance analysis of the proposed antenna is examined by varying the folded slot length ls_4 and ls_8, which plays an important role in determining the resonant frequencies at L_1 and L_2. When the ls_4 is varied from 9.4 mm to 10.6 mm in step 0.2 mm, the resonant frequencies at L_1 and L_2 shift from lower to higher values, with the optimum value found to be 10 mm, as shown in Fig. 9(a).

Similarly, Fig. 9(b) observes the resonance frequency shift when the ls8 is varied from 21.1 mm to 21.4 mm with a step size of 0.05 mm and the optimized value is 21.25 mm.

IV. RESULTS AND DISCUSSION

A. EXPERIMENTAL RESULTS

The S-parameters of the fabricated antenna are measured using an Agilent N5230A vector network analyser. A 50 Ω SMA connector is placed at the excitation terminal to provide the input source to the antenna. Fig. 10(a) shows the measured and simulated S- parameters of the proposed antenna, where dual-band resonances are observed at f1 and f2, with impedance bandwidths for $|S_{11}| < -10$ dB in the ranges of 1615-1675 MHz (3.6%) for L_1 and 1055-1380 MHz (26.7 %) for L_2, respectively.

A small deviation between the simulated and measured values may be attributed to the fabrication and soldering processes. The far-field radiation performance parameters, such as gain and axial ratios, are measured and shown in

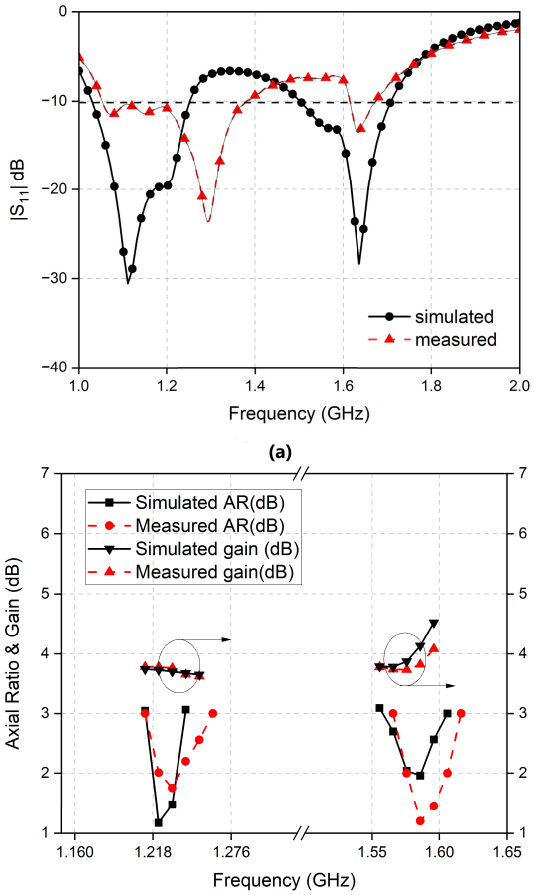

FIGURE 10. (a) Simulated and measured S-parameters, (b) AR and gain response.

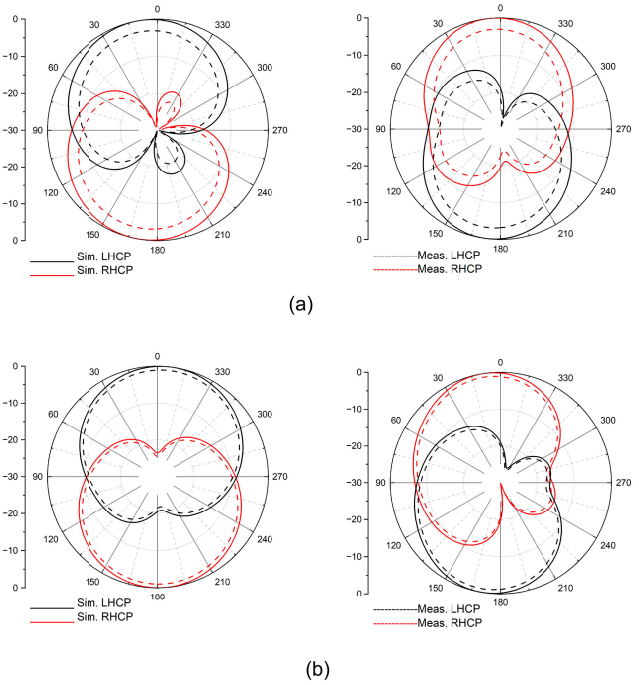

FIGURE 11. Simulated and measured radiation pattern for $L1$ and $L2$ at a) $\theta = 0°$, $\phi = 0°$, b) $\theta = 0°$, $\phi = 90°$.

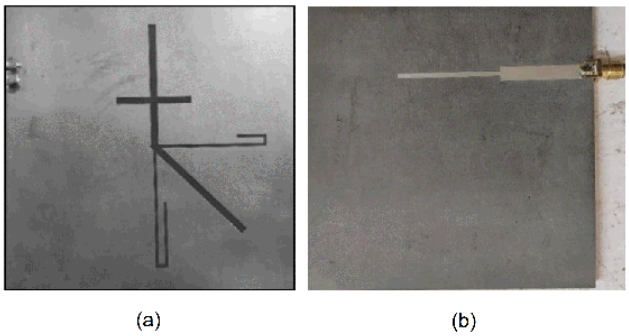

FIGURE 12. Photograph of the fabricated CP slot antenna. (a) Top view. (b) Bottom view.

Fig. 10(b). The minimum axial ratios are found at 1.232 GHz of 1.75 dB and 1.585 GHz of 1.2 dB. The lower operating frequency ranges are 4.04 % (1212-1262 MHz) for L2 and 3.2 % (1565-1616 MHz) for L1, with maximum gains of 3.8 dBic and 4.1 dBic, respectively. The simulated radiation efficiency is 81.1 % and 80.7 % at frequencies 1.227 GHz and 1.575 GHz respectively. The proposed antenna's simulated and measured radiation patterns at 1.227 GHz and 1.575 GHz are shown in Fig. 11. The radiated field is towards the broadside direction that maintains minimum cross-polarization levels between the frequencies. The proposed design is fabricated, and the top and bottom view images are shown in Fig. 12.

B. PERFORMANCE ANALYSIS

Table 2 presents a performance comparison analysis of antennas reported with small frequency ratios for dual-band dual-CP applications. In [25], although the design exhibits better performance in terms of ARBW and gain, its larger size is attributed to the generation of higher-order modes compared to the proposed antenna's resonance frequencies and dimensions. The works in [27] and [31] utilized annular ring antennas with parasitic elements, leading to complicated structures with reduced ARBW and IBW compared to the proposed approach. Furthermore, both designs employ substrate thicknesses nearly double that of the proposed antenna. The design in [14] uses two substrate layers with a large separation between the radiating layer and the ground plane, resulting in installation challenges despite outperforming the proposed work. The single-layer antenna array in [32], with a small frequency ratio, demonstrates the large size and low IBW and ARBW. Substrate layer thickness in [34] is larger with frequency ratio compared to the proposed work. Hence, the proposed antenna is designed with single-layer, single-fed, single-element with a small frequency ratio to meet the specifications for GPS applications, achieving adequate bandwidth and gain values.

TABLE 2. Comparison analysis with previously reported Dual band CP antennas.

Ref	Antenna Size (λ_o^3)	Frequency (GHz)	Feed	No of Layers	IBW (%)	3-dB ARBW (%)	Gain (dBic)	Frequency Ratio
[25]	0.88 x 0.9 x0.0084	2.84/3.58	Microstrip line	1	15/9.7	3.1/1.8	4.47/4.23	1.27
[26]	0.35 x 0.35 x 0.013	1.176/1.575	Coaxial feed	2	2.5/2.7	1.5/1	3.68/3.3	1.34
[31]	0.298 x 0.298 x 0.026	1.227/1.575	Proximity coupled feed	1	6.1/3.7	1/1	2.22/1.14	1.28
[14]	0.33 x 0.33 x 0.1227	1.227/1.575	T-shaped coaxial feed	2	40.7	6.56/7.74	7.72/8.11	1.28
[32]	1.44 x 1.44 x 0.024	2.4/2.68	Microstrip feed	1	3.3/2.6	0.9/0.3	11.7/11.8	1.17
[34]	0.9735 x 0.9735 x 0.082	3.245/4.3	Aperture coupled feed	2	12.7/13	2.47/1.17	8.51/8.6	1.33
This Work	0.425 x0.425 x 0.0068	1.227/1.575	Microstrip line	1	26.7/3.6	4.04/3.2	3.8/4.1	1.28

λ_o- corresponding to the center frequency of the lower band

V. CONCLUSION

This work presents a novel dual-band, dual-circularly polarized (CP) slot antenna with two minimum axial ratios (ARs) under two pairs of orthogonal polarizations with opposite rotations. A conventional narrow slot structure is excited by two resonant modes with in-phase and anti-phase characteristics, respectively. Additional resonant modes, orthogonal to the initial resonant modes, are created by adding folded slots without utilizing higher-order modes to achieve left-hand circular polarization (LHCP) and right-hand circular polarization (RHCP), respectively. To verify the proposed design concept, a prototype is fabricated and measured. The simulated and measured results agree with slight deviations, confirming dual polarizations at 1.227 GHz and 1.575 GHz, with gains of 3.8 dBic and 4.1 dBic achieved, respectively. The proposed design employs the concept of orthogonal mode creation in proximity to existing resonant modes, utilizing a single feed, a simple structure, and single radiator properties, making it attractive for modern communication systems.

ACKNOWLEDGMENT

The authors express their sincere gratitude to R. Sudha, Laboratory Instructor of the Antenna and Microwave Laboratory, Amrita School of Engineering, Coimbatore, for her assistance with antenna measurements.

REFERENCES

[1] D. M. Pozar and S. M. Duffy, "A dual-band circularly polarized aperture-coupled stacked microstrip antenna for global positioning satellite," *IEEE Trans. Antennas Propag.*, vol. 45, no. 11, pp. 1618–1625, Nov. 1997.

[2] S. Gao, Q. Luo, and F. Zhu, *Circularly Polarized Antennas*. Hoboken, NJ, USA: Wiley, 2013.

[3] P. K. T. Rajanna, K. Rudramuni, and K. Kandasamy, "A wideband circularly polarized slot antenna backed by a frequency selective surface," *J. Electromagn. Eng. Sci.*, vol. 19, no. 3, pp. 166–171, Jul. 2019.

[4] Z.-P. Zhong, X. Zhang, J.-J. Liang, C.-Z. Han, M.-L. Fan, G.-L. Huang, W. Xu, and T. Yuan, "A compact dual-band circularly polarized antenna with wide axial-ratio beamwidth for vehicle GPS satellite navigation application," *IEEE Trans. Veh. Technol.*, vol. 68, no. 9, pp. 8683–8692, Sep. 2019.

[5] S. M. Kim, K. S. Yoon, and W. G. Yang, "Dual-band circular polarization square patch antenna for GPS and DMB," *Microw. Org. Technol. Lett.*, vol. 49, no. 12, pp. 2925–2926, 2007.

[6] C. Wang, J. Li, A. Zhang, W. T. Joines, and Q. H. Liu, "Dual-band capacitively loaded annular-ring slot antenna for dual-sense circular polarization," *J. Electromagn. Waves Appl.*, vol. 31, no. 9, pp. 867–878, Jun. 2017.

[7] X. Sun, Z. Zhang, and Z. Feng, "Dual-band circularly polarized stacked annular-ring patch antenna for GPS application," *IEEE Antennas Wireless Propag. Lett.*, vol. 10, pp. 49–52, 2011.

[8] J. Li, J. Shi, L. Li, T. A. Khan, J. Chen, Y. Li, and A. Zhang, "Dual-band annular slot antenna loaded by reactive components for dual-sense circular polarization with flexible frequency ratio," *IEEE Access*, vol. 6, pp. 64063–64070, 2018.

[9] C. Deng, Y. Li, Z. Zhang, G. Pan, and Z. Feng, "Dual-band circularly polarized rotated patch antenna with a parasitic circular patch loading," *IEEE Antennas Wireless Propag. Lett.*, vol. 12, pp. 492–495, 2013.

[10] Y. Xu, L. Zhu, and N.-W. Liu, "Differentially fed wideband filtering slot antenna with endfire radiation under multi-resonant modes," *IEEE Trans. Antennas Propag.*, vol. 67, no. 10, pp. 6650–6655, Oct. 2019.

[11] Y. Yoshimura, "A microstripline slot antenna," *IEEE Trans. Microw. Theory Techn.*, vol. MTT-20, no. 11, pp. 760–762, Nov. 1972.

[12] C.-H. Chen and E. K. N. Yung, "Dual-band circularly-polarized CPW-fed slot antenna with a small frequency ratio and wide bandwidths," *IEEE Trans. Antennas Propag.*, vol. 59, no. 4, pp. 1379–1384, Apr. 2011.

[13] W.-T. Hsieh, T.-H. Chang, and J.-F. Kiang, "Dual-band circularly polarized cavity-backed annular slot antenna for GPS receiver," *IEEE Trans. Antennas Propag.*, vol. 60, no. 4, pp. 2076–2080, Apr. 2012.

[14] S. Lee, Y. Yang, K.-Y. Lee, and K. C. Hwang, "Dual-band circularly polarized annular slot antenna with a lumped inductor for GPS application," *IEEE Trans. Antennas Propag.*, vol. 68, no. 12, pp. 8197–8202, Dec. 2020.

[15] R. Xu, J.-Y. Li, J. Liu, S.-G. Zhou, Z.-J. Xing, and K. Wei, "A design of dual-wideband planar printed antenna for circular polarization diversity by combining slot and monopole modes," *IEEE Trans. Antennas Propag.*, vol. 66, no. 8, pp. 4326–4331, Aug. 2018.

[16] Q. Wu, J. Yin, C. Yu, H. Wang, and W. Hong, "Low-profile millimeter-wave SIW cavity-backed dual-band circularly polarized antenna," *IEEE Trans. Antennas Propag.*, vol. 65, no. 12, pp. 7310–7315, Dec. 2017.

[17] Y. Xu, L. Zhu, and N. Liu, "A foldedhigher-modeslot antenna with enhanced bandwidth and radiation pattern reshaping," *Int. J. RF Microw. Comput.-Aided Eng.*, vol. 31, no. 9, p. 22721, Sep. 2021.

[18] X. L. Bao and M. J. Ammann, "Monofilar spiral slot antenna for dual-frequency dual-sense circular polarization," *IEEE Trans. Antennas Propag.*, vol. 59, no. 8, pp. 3061–3065, Aug. 2011.

[19] R. Garbacz and R. Turpin, "A generalized expansion for radiated and scattered fields," *IEEE Trans. Antennas Propag.*, vol. AP-19, no. 3, pp. 348–358, May 1971.

[20] R. Harrington and J. Mautz, "Computation of characteristic modes for conducting bodies," *IEEE Trans. Antennas Propag.*, vol. AP-19, no. 5, pp. 629–639, Sep. 1971.

[21] J. J. Borchardt and T. C. Lapointe, "U-slot patch antenna principle and design methodology using characteristic mode analysis and coupled mode theory," *IEEE Access*, vol. 7, pp. 109375–109385, 2019.

[22] K. R. Schab, J. M. Outwater, M. W. Young, and J. T. Bernhard, "Eigenvalue crossing avoidance in characteristic modes," *IEEE Trans. Antennas Propag.*, vol. 64, no. 7, pp. 2617–2627, Jul. 2019.

[23] S. Ghosal, R. Sinha, A. De, A. Chakrabarty, and H. Son, "Theory of coupled characteristic modes," *IEEE Trans. Antennas Propag.*, vol. 68, no. 6, pp. 4677–4687, Jun. 2020.

[24] H. Haus and W. P. Huang, "Coupled-mode theory," *Proc. IEEE*, vol. 79, no. 10, pp. 1505–1518, Oct. 1991.

[25] K. R. Schab and J. T. Bernhard, "A group theory rule for predicting eigenvalue crossings in characteristic mode analyses," *IEEE Antennas Wireless Propag. Lett.*, vol. 16, pp. 944–947, 2017.

[26] Y. Xu, L. Zhu, and N.-W. Liu, "Design approach for a dual-band circularly polarized slot antenna with flexible frequency ratio and similar in-band gain," *IEEE Antennas Wireless Propag. Lett.*, vol. 21, pp. 1037–1041, 2022.
[27] C. Sahana, N. Devi, and M. Jayakumar, "Dual-band circularly polarized annular ring patch antenna for GPS-aided GEO-augmented navigation receivers," *IEEE Antennas Wireless Propag. Lett.*, vol. 21, pp. 1737–1741, 2022.
[28] M. M. Kartha and M. Jayakumar, "Circularly polarized stub-loaded annular ring patch antenna for 2×2 MIMO satellite application," *Measurement*, vol. 217, Aug. 2023, Art. no. 113044.
[29] S. J. Vignesh and S. Natarajamani, "A novel meandered line MIMO antenna for 5G mobile terminals for N-77 band wireless communications," in *Proc. Int. Conf. Microw., Opt., Commun. Eng. (ICMOCE)*, May 2023, pp. 1–4.
[30] V. Mekaladevi, N. Devi, and M. Jayakumar, "Design and performance analysis of SIW cavity-backed sectored slot antenna for ISM band applications," in *Proc. 6th Int. Conf. Wireless Commun., Signal Process. Netw. (WiSPNET)*, Mar. 2021, pp. 126–129.
[31] N. Pham, J.-Y. Chung, and B. Lee, "A proximity-fed antenna for dual-band gps receiver," *Prog. Electromagn. Res. C*, vol. 61, pp. 1–8, 2016.
[32] Q.-S. Wu, X. Zhang, L. Zhu, J. Wang, G. Zhang, and C.-B. Guo, "A single-layer dual-band dual-sense circularly polarized patch antenna array with small frequency ratio," *IEEE Trans. Antennas Propag.*, vol. 70, no. 4, pp. 2668–2675, Apr. 2022.
[33] N. Behdad and K. Sarabandi, "Dual-band reconfigurable antenna with a very wide tunability range," *IEEE Trans. Antennas Propag.*, vol. 54, no. 2, pp. 409–416, Feb. 2006.
[34] W.-W. Chen, Q.-S. Wu, and X. Zhang, "Quad-mode dual-band dual-sense circularly polarized microstrip patch antenna," *IEEE Antennas Wireless Propag. Lett.*, vol. 23, pp. 1503–1507, 2024.

MEKALADEVI V (Graduate Student Member, IEEE) received the B.E. degree from Periyar University, India, in 2003, and the M.Tech. degree from Amrita Vishwa Vidyapeetham, in 2013. She is currently a Research Scholar at Amrita Vishwa Vidyapeetham. Her research interest includes dual-polarized antennas for wireless communication applications.

NATARAJAMANI S (Member, IEEE) received the B.E. and M.E. degrees from Anna University, India, in 2005 and 2007, respectively, and the Ph.D. degree from the National Institute of Technology, Rourkela, India, in 2014. He is currently an Assistant Professor with the Department of Electronics and Communication Engineering, Amrita Vishwa Vidyapeetham, Coimbatore, India. His current research interest includes planar antennas for wireless applications.